Extremely anisotropic scintillations

M. A. Walker,[1]★A. G. de Bruyn[2,3] and H. E. Bignall[4,5]

[1]*Manly Astrophysics, Unit 3, 22 Cliff Street, Manly, NSW 2095, Australia*
[2]*Netherlands Institute for Radio Astronomy, PO Box 2, 7990 AA Dwingeloo, the Netherlands*
[3]*Kapteyn Astronomical Institute, University of Groningen, PO Box 800, 9700 AV Groningen, the Netherlands*
[4]*Joint Institute for VLBI in Europe, Postbus 2, 7990AA Dwingeloo, the Netherlands*
[5]*Curtin Institute of Radio Astronomy, Curtin University of Technology, GPO Box U1987, Perth, WA 6845, Australia*

ABSTRACT

A small number of quasars exhibit interstellar scintillation on time-scales less than an hour; their scintillation patterns are all known to be anisotropic. Here, we consider a totally anisotropic model in which the scintillation pattern is effectively one-dimensional. For the persistent rapid scintillator J1819+3845, we show that this model offers a good description of the two-station time-delay measurements and the annual cycle in the scintillation time-scale. Generalizing the model to finite anisotropy yields a better match to the data but the improvement is not significant and the two additional parameters which are required to describe this model are not justified by the existing data. In contrast, our data for the persistent rapid scintillator PKS1257−326 are significantly better fit by a two-dimensional model with a major-to-minor axis ratio of 6 for the scintillation pattern. For J1819+3845, the totally anisotropic model predicts that the particular radio flux variations seen between mid-July and late August should repeat between late August and mid-November, and then again between mid-November and late December as the Earth twice changes its direction of motion across the scintillation pattern. If this effect can be observed then the minor-axis velocity component of the screen and the orientation of that axis can both be precisely determined. In reality, the axis ratio is finite, albeit large and spatial decorrelation of the flux pattern along the major axis may be observable via differences in the pairwise fluxes within this overlap region; in this case, we can also constrain both the major-axis velocity component of the screen and the magnitude of the anisotropy.

Key words: scattering – turbulence – ISM: structure.

1 INTRODUCTION

There are three quasars which are known to exhibit large-amplitude radio flux variations on time-scales of less than an hour: PKS0405−385 (Kedziora-Chudczer et al. 1997), whose variations are intermittent, and the persistent variables PKS1257−326 (Bignall et al. 2003) and J1819+3845[1] (Dennett-Thorpe & de Bruyn 2000). The short time-scale and the strong frequency dependence of the observed variations indicate that interstellar scintillation is the cause (Kedziora-Chudczer et al. 1997). This conclusion is compellingly reinforced by the observed annual cycle in variability time-scale which is effected by the rotation of the Earth's orbital velocity vector (Bignall et al. 2003; Dennett-Thorpe & de Bruyn 2003). Sim-

ilarly, the two-station time-delay measurements (Dennett-Thorpe & de Bruyn 2002; Bignall et al. 2006) explicitly demonstrate the spatial modulation of flux which is inherent in scintillation. The annual cycle in the characteristic time-scale of the scintillations provides strong constraints on the velocity of the scattering material; in turn this constrains the distance to the scattering screen if one identifies the scintillation time-scale with the time taken to cross a Fresnel zone. Better constraints on the screen distance are obtained by constructing models and attempting to match them to all aspects of the data for a given source; the distances deduced in this way are surprisingly small – of order 10 pc from the Earth (Bignall et al. 2003; Dennett-Thorpe & de Bruyn 2003) – so very high brightness temperatures are not required for the sources.

The same annual cycle in the scintillation time-scale also provides evidence for strong anisotropy in the scintillation pattern (Bignall et al. 2003; Dennett-Thorpe & de Bruyn 2003). The scintillation time-scale is affected by both anisotropy in the scattering material and in the source structure. Quasars often exhibit elongated structure ('jets') on milliarcsecond and larger scales (e.g. Walker,

★E-mail: mark.walker@mawtech.com.au
[1]In a recent analysis of data taken in 2008 March, it was discovered that J1819+3845 had ceased to vary on short time-scales (Cimo & de Bruyn, personal communication).

Benson & Unwin 1987) so it is likely that they do have elongated structure on the sub-milliarcsecond angular scales relevant to interstellar scintillation. However, the spectral purity of the observed light curves – that is their quasi-sinusoidal nature – argues that the scattering screens must also have anisotropic structure (Rickett, Kedziora-Chudczer & Jauncey 2002; see also Bignall et al. 2003), and that the major-to-minor axis ratio is large (>4). Unfortunately, the spectral purity of the light curves does not offer a sensitive test of the level of anisotropy once the axis ratio becomes large.

Because they are so nearby, yet they produce large amplitude variations, we know that the screens responsible for intra-hour variability in quasars must be regions of very strong scattering – i.e. they must scatter radio-waves through large angles. Thus, if the local interstellar medium is representative then similar, more distant screens could make a substantial contribution to the total scattering seen on other lines of sight. For compact radio quasars, this suggests that smaller amplitude variability on longer time-scales should be relatively common and this expectation is qualitatively consistent with the results of flux monitoring of large numbers of compact extragalactic radio sources (Lovell et al. 2003).

A further indication that similar screens are widely distributed in the Galaxy is the observation of parabolic arcs in the 'secondary spectra' (power spectra of the dynamic spectra) of radio pulsars (Stinebring et al. 2001). Modelling of this phenomenon indicates that localized, strongly scattering screens are responsible, that the scattering is anisotropic and that the screens are hundreds of parsec distant from the Sun (Stinebring et al. 2001; Walker et al. 2004; Cordes et al. 2006; Putney & Stinebring 2006). It therefore seems that the three known intra-hour variable quasars can offer insights into the structure of the broader interstellar medium and it is important that we understand as much as we can about the properties of these nearby scattering screens.

As we have just noted, it is already clear that the major-to-minor axis ratio of the scintillation patterns is large for the three intra-hour variable quasars. Here, we seek to determine whether existing data admit the possibility of the patterns being so anisotropic that the behaviour is effectively one-dimensional and, if so, whether that is the preferred model. In Section 2, we use published data on the annual cycle in scintillation time-scale and the two-station time-delay experiments for both J1819+3845 and PKS1257−326 to test our models. We find that infinite anisotropy in the scintillation pattern is consistent with and slightly preferred by existing data for J1819+3845, but not for PKS1257−326 where a two-dimensional model with an axis ratio of 6 fits the data significantly better than a one-dimensional model. In Section 3, we note the implication that the observed anisotropy for J1819+3845 is primarily due to anisotropy in the scattering screen; we further note that extreme flux-pattern anisotropy leads us to expect the J1819+3845 light curves seen at one time of year to repeat at two other times, as the observer moves back-and-forth across the same region of the scintillation pattern. If the major-to-minor axis ratio of the pattern is $R \lesssim 10^5$ then spatial decorrelation along the major-axis direction may be measurable and flux monitoring of J1819+3845 can then be used to determine the length-scales and velocity components of the screen along both major- and minor-axis directions.

2 MODEL FITTING

We attempted to fit the data for each of the persistent scintillators with both one- and two-dimensional scintillation models. Our two-dimensional model is the one given in Bignall et al. (2006). Five free parameters are needed to characterize the model, they are: the orientation angle, β, of the major axis of the flux-pattern anisotropy; the steady velocity, $\boldsymbol{v}$, with components $v_\parallel$, $v_\perp$ parallel and perpendicular, respectively, to this major axis direction; the characteristic length-scale, $a_\perp$, of the flux pattern measured along its minor axis and the ratio, R, of major-to-minor axis length scales ($R = a_\parallel/a_\perp$). Henceforth, we use the $\parallel$, $\perp$ notation to indicate any vector components resolved on to the major and minor axes of the scintillation pattern; these axes lie in the plane perpendicular to the direction to the source.

The orbital velocity of the Earth, $\boldsymbol{u}_\oplus$, contributes to the total effective velocity of the observer across the scintillation pattern $\boldsymbol{V} := \boldsymbol{u}_\oplus + \boldsymbol{v}$, and in terms of these quantities the annual cycle in scintillation time-scale, t_s, expected in any model is given by

$$t_s = \frac{R a_\perp}{\sqrt{V_\parallel^2 + R^2 V_\perp^2}}, \tag{1}$$

and the time-delay measured between two stations separated by a baseline $\boldsymbol{b}$ is

$$\tau = \frac{b_\parallel V_\parallel + R^2 b_\perp V_\perp}{V_\parallel^2 + R^2 V_\perp^2}. \tag{2}$$

Our one-dimensional scattering model corresponds to the limit of infinite axis ratio ($R \to \infty$) and is completely specified by three of these five parameters: β, $v_\perp$, $a_\perp$. The time-scale and two-station delay in this model are just $t_s = a_\perp/|V_\perp|$ and $\tau = b_\perp/V_\perp$.
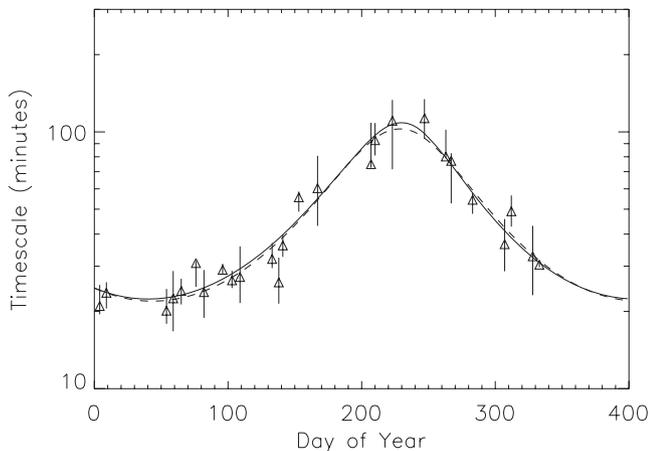
2.1 PKS1257−326

The time-scale and delay data for this source are presented in Bignall et al. (2006). We have confined our attention to the 4.8 GHz data as these are expected to be slightly less affected by atmospheric phase and opacity fluctuations than the 8.5 GHz data. We therefore use the time-delay data reported in column 1, table 1 of Bignall et al. (2006), with the effective UT of each measurement taken as the mid-point of the intervals plotted in their fig. 1 (i.e. 7^h, 15^h, 11^h for May, January and March, respectively). It is not necessary to assign a precise UT to each delay measurement because Bignall et al. (2006) found no detectable variation in the delay over the course of each of their observations. As in Bignall et al. (2006), we fit simultaneously to the time-scale and delay, in order to determine which model best fits the data overall, but our approach differs in two respects from theirs. First, as we have just noted, we are using exclusively the 4.8 GHz data. The second point of difference relates to how we weight the delay measurements, relative to the scintillation time-scale measurements, in their contribution to the quality-of-fit estimator, χ^2. Bignall et al. (2006) weighted the set of time-scale data equally with the set of delay measurements, whereas here we weight each of the 26 measurements of time-scale equally with each of the 5 two-station delay measurements – reflecting the fact that similar amounts of data contributed to each measurement.

Our best fits to these data, using both one- and two-dimensional models, are described by the parameters given in Table 1. Error bars on the various parameters correspond to an increase of one in χ^2 relative to the best-fitting value. Our best-fitting one-dimensional model exhibits similar properties to that of the two-dimensional model in respect of the three parameters which are common between the two models. The annual cycle in scintillation time-scale as predicted by each of the best-fitting models is shown in Fig. 1, along with the data. It is inevitable that the χ^2 value for the best-fitting two-dimensional model is smaller than that of the best-fitting one-dimensional model, just because the two-dimensional model has additional parameters which can be adjusted to achieve a better

Table 1. Best-fitting scintillation model parameters (two- and one-dimensional).

Source	β (N → E)	$v_\perp$ (km s^{-1})	$a_\perp$ (Mm)	$v_\parallel$ (km s^{-1})	R	χ^2
1257−326	123°2 (±3°)	18.7 (±0.8)	43.3 (±1.4)	28 (+15, − 10)	6(+2, − 1)	25.0
1257−326	126°6 (±0°6)	20.5 (±0.3)	44.9 (±1)	−	−	31.7
1819+3845	−97°39 (+0°45, −0°65)	19.62 (±0.40)	29.8 (±0.7)	400^a (−354)	176(−153)	50.3
1819+3845	−97°35 (±0°40)	19.67 (±0.24)	29.5 (±0.6)	−	−	52.6

^{a}Fixed at the maximum physically plausible value; the associated error bar corresponds to increasing χ^2 by unity relative to this point.


Figure 1. The annual cycle in scintillation time-scale for PKS1257−326 for best-fitting one- and two-dimensional models (dashed and solid lines, respectively), along with the data.

Figure 2. The χ^2 surface for PKS1257−326 for the parameters $v_\parallel$ and R, shown as a contour plot, for the best-fitting two dimensional models. The best of all of such models has the parameters shown in Table 1, and this plot shows the values of χ^2 relative to that model. Contours are spaced by factors of 2 in $\Delta\chi^2$, starting at 1/8, so the dashed contour shows the parameter error ellipse $\Delta\chi^2 = 1$.

match to the data, but in the present case the two-dimensional model yields a χ^2 value which is significantly better. We can normalize our model χ^2 values by the number of degrees of freedom, bearing in mind that there are 26 time-scale measurements and 5 two-station delay measurements, so 31 constraints in total. The two-dimensional model contains five free parameters whereas the one-dimensional model has only three, implying reduced-χ^2 values of $\chi_r^2 = 0.96$ and 1.13 for two- and one-dimensional models, respectively: the two-dimensional fit is thus preferred.

Fig. 2 shows the χ^2 surface for the two-dimensional model when the parameters R and $v_\parallel$ are varied over a large range (several orders of magnitude in each case). Here, we can see that the best-fitting model is well localized in this space at a confidence level of at least $\Delta\chi^2 = 4$, but at higher confidence levels very large values of R and $v_\parallel$ are permitted as can be seen from the $\Delta\chi^2 = 8$ contour.

Our results for PKS1257−326 differ from those reported in Bignall et al. (2006) where the best-fitting models were found to have substantially larger anisotropies than our preferred value of $R = 6$. The two main differences between their models and ours are (i) a different weighting of the time-delays relative to the time-scale measurements, and (ii) their inclusion of the 8.5 GHz data. We have excluded (i) as the primary cause of the difference because we find that our results do not change significantly if we use the same weighting scheme as Bignall et al. (2006). Thus, we attribute the differences to the influence of the 8.5 GHz data. We expect the differences in atmospheric phase stability and opacity to be small over the frequency range 4.8 GHz to 8.4 GHz, except for rare occasions when the observing conditions are very poor, so it seems unlikely that this is the reason for the difference between the two frequencies. One possible explanation is that for PKS1257−326
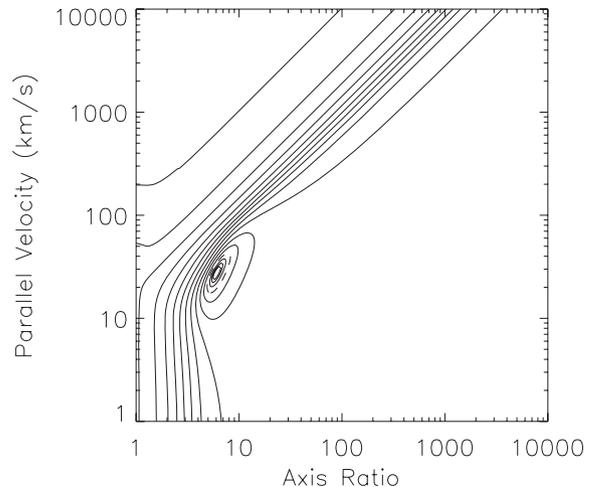
the structure of the flux pattern is significantly influenced by the size of the source, which is expected to be larger at lower frequencies: this might significantly increase $a_\perp$, hence decrease R, at 4.8 GHz. However, Bignall et al. (2006) find $a_\perp$ values for the two frequencies which differ by only ∼20 per cent, so it seems unlikely that this can explain the difference. It remains unclear why the higher frequency data on PKS1257−326 have such a large influence on the outcome of the modelling.

2.2 J1819+3845

For J1819+3845, we use the two station delay observations from 2001 January presented in Dennett-Thorpe & de Bruyn (2002), and the data on annual time-scale variations (time-scale 't_1') given in table 3 of Dennett-Thorpe & de Bruyn (2003). In both of their two-station experiments, Dennett-Thorpe & de Bruyn (2002) clearly measured a change in delay as the VLA-Westerbork baseline rotated during the course of their observations and the sign of the delay changed. We used the measurements as plotted in their fig. 3: on 2001 January 7, $\tau = -94 \pm 4$ s at UT12:14, and $\tau = +107 \pm 4$ s at UT15:54; on 2001 January 12, $\tau = -76 \pm 13$ s at UT11:58, and $\tau = +121 \pm 21$ s at UT16:07. Here, the sign convention is that a positive value of τ means that features in the light curve occur earlier in the VLA data than in the Westerbork data. As for PKS1257−326, we attempt to fit both types of data simultaneously and we do so with both one- and two-dimensional models. In fitting our models to the data, each of the four delay measurements was
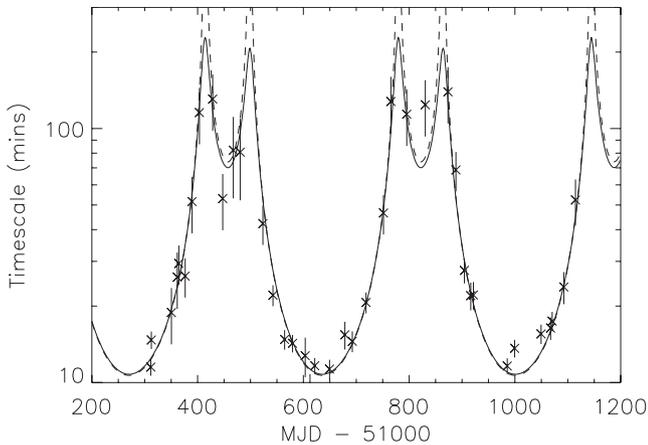
Figure 3. The annual cycle in scintillation time-scale for J1819+3845 for best-fitting one- and two-dimensional models (dashed and solid lines, respectively), along with the data.

Figure 4. The χ^2 surface for J1819+3845 for the parameters $v_\parallel$ and R, shown as a contour plot, for the best-fitting two dimensional models. The best of all such models has an unphysically large value of $v_\parallel$ and in arriving at the parameter values reported in Table 1, we have imposed the restriction $v_\parallel \leq 400$; this limiting velocity is shown with a dotted line here. Contours are spaced by factors of 2 in $\Delta\chi^2$, starting at 1/8, so the dashed contour shows the parameter error ellipse $\Delta\chi^2 = 1$.

given equal weight with each of the 39 time-scale measurements. Our best-fitting two-dimensional model proved to be unphysical, with a superluminal major-axis velocity component. An unphysical solution is of no interest, so we proceeded by fixing the major-axis velocity at the largest physically plausible value, which we chose to be $400 \, \text{km s}^{-1}$ – comparable to the escape speed from the Galaxy. The resulting best-fitting model parameters are given in Table 1, and the corresponding annual cycle in scintillation time-scale is shown in Fig. 3 for both best-fitting models and the data.
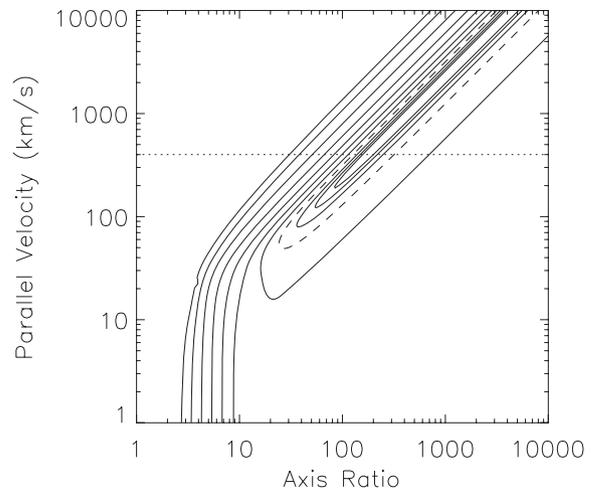
We see that for J1819+3845 the best-fitting one- and two-dimensional models are very similar in respect of the values of the parameters which they have in common, and that they differ only slightly in respect of the predicted scintillation time-scales. The two-dimensional model matches the data a little better, as measured by the χ^2 of the fits, but the reduced χ^2 values are $\chi^2_r = 1.315$ for the one-dimensional model and $\chi^2_r = 1.324$ for the two-dimensional model – indicating that the difference in χ^2 is not significant and the extra two parameters needed for the two-dimensional model are not justified by these data.

This point is underlined by the plot (Fig. 4) of the χ^2 surface for the parameters $(R, v_\parallel)$ belonging only to the two-dimensional model. In this figure, we see that very large values of R and $v_\parallel$ are not only permissible but actually preferred by the data, with a very strong degeneracy in the direction $v_\parallel \propto R$. This plot also demonstrates that pattern anisotropies as small as $R = 4$ can be confidently rejected for this source because the corresponding increase in χ^2 relative to the best-fitting two-dimensional model (Table 1) exceeds $2^5 = 32$.

2.3 Solution geometries

Care is needed to avoid confusion in interpreting the models presented here because the major axis of the scintillation pattern incompletely defines our coordinate axes $(\parallel, \perp)$: there remain ambiguities of sign. To resolve these ambiguities, we present a vector diagram of our best-fitting models in Fig. 5.

For J1819+3845, our preferred (one-dimensional) model yields good agreement with the results of Dennett-Thorpe & de Bruyn (2003) in respect of the orientation of the major-axis and the value of the perpendicular velocity component; this is all that can be expected since the results of Section 2.2 demonstrate that R and $v_\parallel$

cannot be meaningfully constrained by the available data for this source.

Our preferred (two-dimensional) model for PKS1257−326 appears to be consistent with the results of Bignall et al. (2006; their fig. 6) in respect of the orientation of the major-axis and the value of the perpendicular velocity component. Our parameter $v_\parallel = 28 \, \text{km s}^{-1}$ also appears to be broadly consistent with the model shown in their fig. 6 (i.e. their model 'c'), even though that model has a significantly larger axis ratio ($R = 12$) than our solution. We note that Bignall et al. (2006) report a preference for even larger axis ratios, $R \sim 10^2$ (their model 'b'), in their fitting, and that their model 'c' is one in which the axis ratio has been limited to $R \leq 12$.

3 DISCUSSION

The models employed in Section 2 are descriptions of the geometry and kinematics of the scintillation pattern. By virtue of their great distances, which are $\sim 10^8$ times larger than the estimated screen distances, the sources are not expected to contribute significantly to the measured pattern velocities. However, source structure could be important in determining the length-scales $a_\perp$, $a_\parallel$ because the observed pattern is a convolution of the point-source response of the screen with the (demagnified, inverted) source image. The question then arises as to whether the scintillation pattern for J1819+3845 is quasi-one-dimensional because of the source structure or because of the phase structure in the scattering screen? Although extragalactic radio sources commonly exhibit elongated structure ('jets'), the axis ratios of their images are small in comparison with the pattern anisotropies which we are considering for J1819+3845. For example, in the well-studied case of the source 3C120 the jet length:width ratio is less than 10 almost everywhere in a logarithmically broad range of angular scales (Walker et al. 1987), whereas the best-fitting two-dimensional model for J1819+3845 yields a pattern axis ratio of more than 100 (see Table 1). By contrast, the phase screen anisotropy is already known to be large in the case of the rapid scintillators PKS0405−385 and PKS1257−326 (Rickett et al. 2002; Bignall et al. 2006), albeit with a modest lower limit
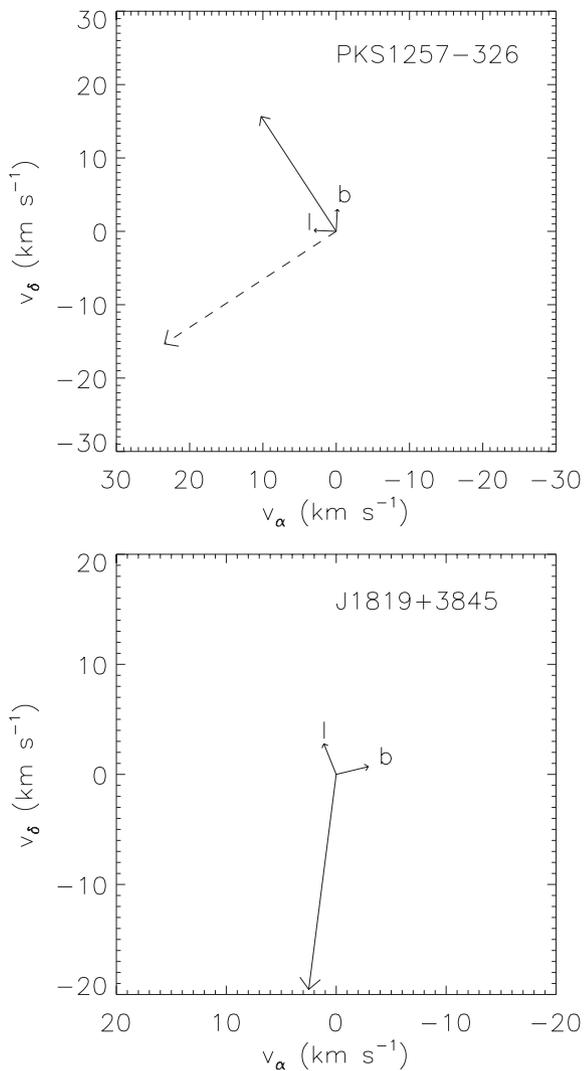
Figure 5. Magnitude and orientation of $v_\perp$ (solid line), $v_\parallel$ (dashed line) for PKS1257−326 (top panel) and $v_\perp$ for J1819+3845 (bottom panel), as determined by the best-fitting model in each case (two-dimensional for PKS1257−326 and one-dimensional for J1819+3845). Also plotted on each figure are vectors corresponding to the local directions of increasing Galactic longitude (*l*) and latitude (*b*).

tent with the high level of spectral purity in the radio light curves of the fast scintillators (Rickett et al. 2002), but that diagnostic test is insensitive to the precise value of R once it becomes large. This raises the question: how can large anisotropies be measured? Fig. 3 demonstrates that when the scintillation time-scale is very long it is sensitive to finite anisotropy, but unfortunately it is also difficult to measure accurately in this case. Indeed, Dennett-Thorpe & de Bruyn (2003) show three light curves (recorded on 1999 August 27, 1999 November 28 and 2000 August 27) for which the variations are very slow and no measurement of scintillation time-scale is reported in their table 3. We now describe an alternative approach to measuring R which can be employed for J1819+3845.

The scintillation time-scale is formally infinite in the one-dimensional scattering model at times when $V_\perp = 0$. (According to our best-fitting totally anisotropic scattering model for J1819+3845, this condition is satisfied each year sometime around August 23rd and again around November 15th.) These points correspond to changes in the sign of $V_\perp$ and they are therefore turning points, $x_{\perp,\text{min}}$, $x_{\perp,\text{max}}$, in the minor-axis coordinate (which we shall denote $x_\perp$). This is illustrated in Fig. 6, where we see that each value of $x_\perp$ in the range $x_{\perp,\text{min}} < x_\perp < x_{\perp,\text{max}}$ occurs at three distinct times each year – once between the two times when $V_\perp$ changes sign, once before this interval and once after. In the totally anisotropic model, the flux depends only on $x_\perp$ so we expect a one-to-one correspondence between fluxes measured before and after the turning
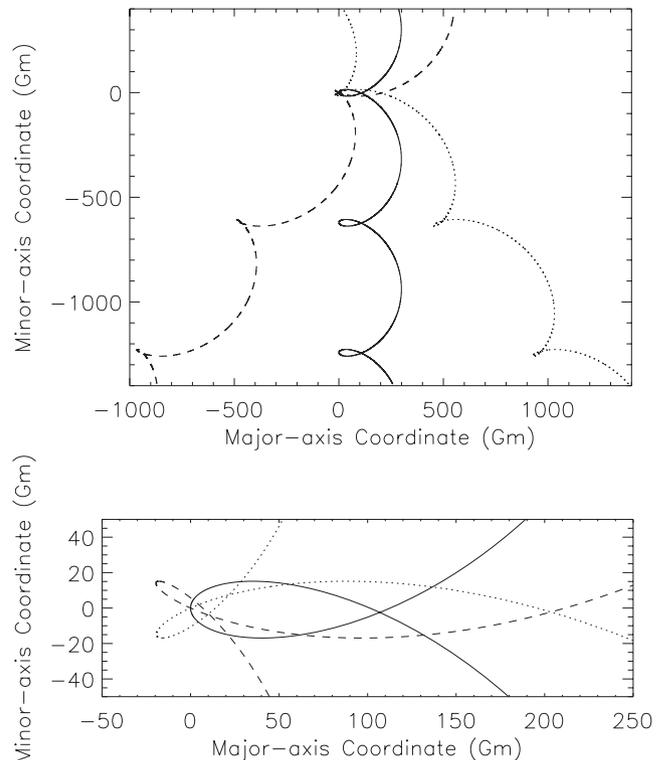
Figure 6. Three possible trajectories of an observer relative to the J1819+3845 scintillation pattern over a roughly three-year interval (top panel): the solid line corresponds to $v_\parallel = 0$; dotted and dashed lines correspond to $v_\parallel = \pm 15\,\text{km s}^{-1}$. The origin of coordinates is arbitrary for each curve. Turning points in the minor-axis coordinate correspond to $V_\perp = 0$ and this condition is satisfied on the same day regardless of $v_\parallel$. These turning points occur in late August and mid-November each year. Each value of the minor-axis coordinate between the turning points occurs on three separate occasions for all possible trajectories. The lower panel shows a close-up of the region around the origin of coordinates in the top panel.

($R > 4$). Consequently, it is natural to interpret our result as extreme anisotropy in the phase screen rather than in the source. In fact, this interpretation is the only possible one because if $a_\parallel \to \infty$ as a result of a very elongated source, then the amplitude of the resulting scintillations should be small because of the smoothing effect of the convolution, whereas it is observed to be large. Thus, the extreme pattern anisotropy which we infer for J1819+3845 requires extremely anisotropic scattering. The likely interpretation of this result is that the scattering takes place in a region where the magnetic field is both strong and highly ordered.

Why go to the bother of testing a one-dimensional scattering model when we know that the real scattering screens must have a finite anisotropy? The point here is one of scale: it is not yet clear what the anisotropy is even to order of magnitude. And it does appear that it can be very large: not only is the one-dimensional model entirely adequate to describe the data for J1819+3845, but the best of all two-dimensional models for this source are those with anisotropy $R > 10^2$. Very large values of the anisotropy are consis-

points, where those measurements are made at the same value of $x_\perp$.

In practice, the anisotropy, R, must be finite albeit large. A consequence of this is that a pair of points with the same value of $x_\perp$ but having major-axis coordinate separations $|\delta x_\parallel| \gtrsim a_\parallel \simeq 30R$ Mm will exhibit significantly different fluxes. The correlation between fluxes taken pair-wise in this way increases as $|\delta x_\parallel|$ decreases and is very strong for $|\delta x_\parallel| \ll a_\parallel$. In this way, we can measure $a_\parallel$ if we know the trajectory $x_\parallel$ as a function of time, which in turn is completely determined by the value of $v_\parallel$. We do not know $v_\parallel$ independently but its value can be determined simultaneously with that of $a_\parallel$ because $v_\parallel$ at the two turning points differs by about $40\,\mathrm{km\,s^{-1}}$ as a result of the different contributions from the Earth's velocity vector.

In Fig. 6, we can find, on each trajectory, separations of up to $|\delta x_\parallel| \sim 10^5$ Mm between points with the same perpendicular coordinate, indicating that for these trajectories we can estimate the major-to-minor axis ratio if its value is $R \lesssim 3 \times 10^3$. Fig. 6 shows three example trajectories, all of which have $|v_\parallel| \leq 15\,\mathrm{km\,s^{-1}}$; if, on the other hand, the magnitude of the parallel velocity component is as great as $400\,\mathrm{km\,s^{-1}}$ then this approach is sensitive to still larger values of the anisotropy: $R \lesssim 10^5$. These estimates have all been carried through in the 'frozen screen' approximation, for which it is meaningful to assign a unique steady velocity $\vec{v}$ to the scintillation pattern. The fact that we are able to find good fits to the existing time-scale and time-delay data for J1819+3845 demonstrates that the model is indeed a valid description of the perpendicular motion, but it might fail on the longer time-scales needed to explore the scintillation pattern along the major axis direction. Departures from the simple kinematic model we have used would provide constraints on any physical model of the scattering media.

While undertaking preliminary work for the sort of studies which we have just outlined, we discovered (Cimo & de Bruyn, personal communication) that J1819+3845 stopped varying at some time prior to March 2008; so for now, at least, it is not possible to test these ideas – we must wait for the variations of J1819+3845 to return. Another possible application is to the source PKS0405−385. The variations of this source are known to be intermittent (Kedziora-Chudczer 2006), lasting only a few months at a time, and this makes it difficult to establish the geometric/kinematic properties of the screen(s) by the sort of fitting techniques we employed in Section 2. However, the latest episode of variations of PKS0405−385 exhibits a large range in scintillation time-scale (Kedziora-Chudczer, personal communication) and may thus be a case where $V_\perp$ vanishes at some times of the year and the screen anisotropy is very large.

4 CONCLUSIONS

At present, there is no evidence for finite anisotropy in the scattering screen responsible for the intra-hour variations of J1819+3845

and only a one-dimensional model is appropriate for this source. By contrast, the data we employed for PKS1257−326 are significantly better fit by a two-dimensional, anisotropic screen with a modest axis-ratio $R \sim 6$. In the case of J1819+3845, a strictly one-dimensional model predicts that the particular scintillations seen between late August and mid-November each year should also be seen before and after this period as the Earth's velocity across the flux pattern changes sign at these times and the observer moves back and forth across the same part of the pattern. If repeating flux patterns can be identified in the data they will permit precise determination of the major-axis orientation and the minor-axis velocity component. To the extent that decorrelation of the pair-wise fluxes can be quantified, we can measure the major-to-minor axis ratio, R, and the major-axis velocity component of the screen. Decorrelation is expected to be observable only if $R \lesssim 10^5$.

REFERENCES

Bignall H. E. et al., 2003, ApJ, 585, 653
Bignall H. E., Macquart J. P., Jauncey D. L., Lovell J. E. J., Tzioumis A. K., Kedziora-Chudczer L., 2006, ApJ, 652, 1050
Cordes J. M., Rickett B. J., Stinebring D. R., Coles W. A., 2006, ApJ, 637, 346
Dennett-Thorpe J., de Bruyn A. G., 2000, ApJ, 529, L65
Dennett-Thorpe J., de Bruyn A. G., 2002, Nat, 415, 57
Dennett-Thorpe J., de Bruyn A. G., 2003, A&A, 404, 113
Kedziora-Chudczer L., 2006, MNRAS, 369, 449
Kedziora-Chudczer L., Jauncey D. L., Wieringa M. H., Walker M. A., Nicolson G. D., Reynolds J. E., Tzioumis A. K., 1997, ApJ, 490, L9
Lovell J. E. J., Jauncey D. L., Bignall H. E., Kedziora-Chudczer L., Macquart J. P., Rickett B. J., Tzioumis A. K., 2003, AJ 126, 1699
Putney M. L., Stinebring D. R., 2006, Chin. J. Astron. Astrophys., 6, 233
Rickett B. J., Kedziora-Chudczer L., Jauncey D. L., 2002, ApJ, 581, 103
Stinebring D. R. et al., 2001, ApJ, 549, L97
Walker M. A., Melrose D. B., Stinebring D. R., Zhang C. M., 2004, MNRAS, 354, 43
Walker R. C., Benson J. M., Unwin S. C., 1987, ApJ, 316, 546

This paper has been typeset from a TeX/LaTeX file prepared by the author.